PM2.5 source apportionment using organic marker-based chemical mass balance modeling

Tian, Yingze; Wang, Xiaoning ; Zhao, Peng ; Shi, Zongbo; Harrison, Roy

DOI:
10.1016/j.atmosenv.2022.119477

Document Version
Publisher's PDF, also known as Version of record

Citation for published version (Harvard):
Tian, Y, Wang, X, Zhao, P, Shi, Z & Harrison, R 2023, 'PM2.5 source apportionment using organic marker-based chemical mass balance modeling: influence of inorganic markers and sensitivity to source profiles', *Atmospheric Environment*, vol. 294, 119477. https://doi.org/10.1016/j.atmosenv.2022.119477

Atmospheric Environment 294 (2023) 119477

Contents lists available at ScienceDirect

Atmospheric Environment

journal homepage: www.elsevier.com/locate/atmosenv

PM2.5 source apportionment using organic marker-based chemical mass balance modeling: Influence of inorganic markers and sensitivity to source profiles

Yingze Tian [a], Xiaoning Wang [a], Peng Zhao [a], Zongbo Shi [b], Roy M. Harrison [b,c,*]

[a] State Environmental Protection Key Laboratory of Urban Ambient Air Particulate Matter Pollution Prevention and Control, College of Environmental Science and Engineering, Nankai University, Tianjin, 300071, China
[b] School of Geography Earth and Environmental Science, University of Birmingham, Edgbaston, Birmingham, B15 2TT, UK
[c] Department of Environmental Sciences, Faculty of Meteorology, Environment and Arid Land Agriculture, King Abdulaziz University, Jeddah, Saudi Arabia

HIGHLIGHTS

- A Chemical Mass Balance model is applied to particulate matter from Chengdu, China.
- Inclusion of both inorganic and organic source tracers gives better results.
- There is considerable sensitivity to organic source profiles adopted.
- Recent, locally sampled source profiles give the best outcomes.

GRAPHICAL ABSTRACT

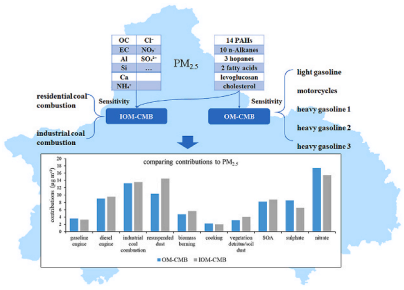

ARTICLE INFO

Keywords:
Particulate matter
Source apportionment
CMB based on organic markers only (OM-CMB)
CMB based on a combination of organic and inorganic markers (IOM-CMB)

ABSTRACT

A Chemical Mass Balance (CMB) model has been applied to source apportionment of $PM_{2.5}$ in the Chinese megacity of Chengdu. The study explored the sensitivity of the CMB model to the adoption of different organic source profiles, and to the use of organic markers only (OM-CMB), compared with using a combination of organic and inorganic markers (IOM-CMB). A comprehensive comparison of OM-CMB and IOM-CMB shows that $PM_{2.5}$ mass concentrations from gasoline vehicles, diesel vehicles, industrial coal combustion, biomass burning, cooking, and SOA which shared same markers in the two methods are in fair to good agreement between the two methods, with the relative biases ranging from 2.2% to 17.3%. The average contributions of sulfate and nitrate sources are more sensitive to the choice of model because inorganic ions were not inputted directly into the OM-CMB. The temporal variations of $PM_{2.5}$ contributions from sulfate, nitrate, SOA, gasoline vehicles, and biomass burning, characterized by unique markers and low collinearity, were in good agreement between the OM-CMB and IOM-CMB results with the Pearson's r above 0.91 ($p < 0.01$). However, resuspended dust estimates from OM-CMB had a relatively weak correlation with that from IOM-CMB (Pearson's $r = 0.73$, $p < 0.01$), due to the different tracers used. When replacing the source profile for industrial coal combustion with that for residential sources, the contributions of resuspended dust and residential coal combustion were higher, and the contributions of other sources were lower compared with the result for the industrial coal combustion. Different source profiles for gasoline vehicles showed considerable sensitivity of the model to the choice of source profile, even

* Corresponding author. School of Geography Earth and Environmental Science, University of Birmingham, Edgbaston, Birmingham, B15 2TT, UK.
E-mail address: r.m.harrison@bham.ac.uk (R.M. Harrison).

https://doi.org/10.1016/j.atmosenv.2022.119477
Received 4 July 2022; Received in revised form 1 November 2022; Accepted 8 November 2022
Available online 14 November 2022

when using data from within a single emissions study. Our results emphasize the value of combining inorganic and organic tracers in minimizing error, and in using up-to-date locally-relevant source profiles in source apportionment of PM.

1. Introduction

Atmospheric fine particles ($PM_{2.5}$) have long been shown to have pronounced effects on human health, air quality, and climate change (Bell et al., 2014; Aguilera et al., 2021; Weber, 2020; Li et al., 2022; Wen et al., 2022). $PM_{2.5}$ is comprised of a complex mixture of chemical components, including both inorganic and organic components (Daellenbach et al., 2020; Thurston et al., 2022). As a significant constituent of $PM_{2.5}$, organic matter (OM) is comprised of thousands of compounds which show distinctive physical and chemical properties (Robinson et al., 2007; Zhang et al., 2013; Zhao et al., 2013). It has been shown that organic molecular markers in the PM, such as n−alkanes, polycyclic aromatic hydrocarbons (PAHs), hopanes, levoglucosan (LEVOG), carboxylic acids, cholesterol (CHOL) and so on, can assist in distinguishing PM sources (Oros and Simoneit, 2000; Ke et al., 2008; Pereira et al., 2017). What's more, simultaneously detecting the organic compounds and inorganic components (elements, ions and carbon fractions) of $PM_{2.5}$ can provide more information towards source identification (Harrison et al., 1996).

To design effective $PM_{2.5}$ reduction strategies in polluted regions currently and to reduce the health burden attributable to ambient PM pollution (Faridi et al., 2022), more refined and accurate source apportionment results for $PM_{2.5}$ are urgently needed. Many studies have estimated the potential source contributions to $PM_{2.5}$ in megacities using various methods, such as receptor models (Huang et al., 2014; Lu et al., 2018; Song et al., 2021), and air quality models (Li et al., 2020; McDuffie et al., 2021). Receptor models are useful tools for source apportionment based on the $PM_{2.5}$ chemical composition. Receptor models can be classified into two main classes: i) Chemical Mass Balance (CMB) model, and ii) multivariate factor analysis models, including Principal Component Analysis/Multiple Linear Regression (PCA/MLR), UNMIX, and Positive Matrix Factorization (PMF). Factor analysis models extract source profiles and their contributions over sets of receptor samples without inputting source profiles, so they require a relatively large number of receptor samples, and sources were identified according to the assessment of mathematical parameters and evaluation of the physical reality of the factor profiles (Xu et al., 2021a). PMF is generally recognized as the superior model in this class as it uses weightings to accord the greatest importance to those variables measured with the lowest uncertainty. The CMB model needs both the measured data of receptor and the source profiles, so the physical meaning of the source categories is clearer. A detailed intercomparison using data from Beijing concluded that CMB gave the most detailed and plausible results compared to PMF (Xu et al., 2021b). The CMB has been used for source apportionment of PM at many locations, worldwide (Zheng et al., 2002; Perrone et al., 2012; Yin et al., 2015; Wu et al., 2020; Wong et al., 2021).

Multicollinearity, arising when two different sources have similar profiles, often disturbs the estimation of the CMB modeling. For $PM_{2.5}$ source categories characterized by specific organic tracers but no specific inorganic tracers, or characterized by large fractions of organic components and few inorganic components, the CMB model with the input of inorganic species only is unable to reliably predict the source contributions. For example, to estimate the contributions from food cooking and vegetative detritus, and to distinguish gasoline vehicles and diesel vehicles, organic markers need to be included in the CMB modeling. Organic molecular markers have consequently been used widely in source apportionment studies (Marmur et al., 2006; Schauer and Cass, 2000; Schauer et al., 1996; Robinson et al., 2006; Chow et al., 2007; Arhami et al., 2018; Esmaeilirad et al., 2020; Tian et al., 2021a; Mancilla et al., 2021). An organic molecular marker-based chemical mass balance (OM-CMB) method has been used to quantify source contributions to carbonaceous aerosols (Ke et al., 2008; Perrone et al., 2012; Villalobos et al., 2017; Lu et al., 2018; Xu et al., 2021a). The OM-CMB method performs well in the source apportionment of organic carbon (OC), but the source contributions to $PM_{2.5}$ are typically calculated by the multiplication of the OC contributions by the ratios of OC to $PM_{2.5}$ mass in the source profiles, and it does not directly estimate contributions of inorganic secondary ions when apportioning $PM_{2.5}$ sources because the inorganic species are not inputted in the CMB modeling (Ke et al., 2008; Xu et al., 2021a). If a combination of inorganic and organic markers is used in the CMB modeling (IOM-CMB), the contributions to $PM_{2.5}$ of all source categories can be directly estimated, but this method has not been widely used. Thus, it is advantageous to explore using a combination of inorganic and organic markers in the CMB modeling of $PM_{2.5}$ through comparing the IOM-CMB modeling based on a combination of organic and inorganic markers with the more conventional OM-CMB modeling based on organic markers only.

In addition, several studies have applied the OM-CMB model for source apportionment of PM in China (Zheng et al., 2005; Liu et al., 2016; Guo et al., 2013; Wang et al., 2009; Xu et al., 2021a). However, the organic source profiles they used were mainly derived from measurements made in the United States, which may be less representative of the local sources and current conditions of the sources in China. Xu et al. (2021a) used the organic source profiles determined in China to ensure that the source profiles used in the CMB model are representative. The CMB results may vary when using different source profiles, so it is necessary to study the influence of adopting different organic and inorganic source profiles on the CMB modeling, namely the sensitivity of CMB to source profiles, so as to investigate the value of using local and updated organic and inorganic source profiles.

Therefore, this paper aims at exploring using a combination of inorganic and organic markers in the CMB modeling of $PM_{2.5}$, and the influence of adopting different organic source profiles. $PM_{2.5}$ source apportionment was conducted by CMB modeling based on organic markers (OM-CMB) and by a combination of organic and inorganic markers (IOM-CMB). Commonly used markers (including OC, elemental carbon (EC), ions, elements) and organic markers (including polycyclic aromatic hydrocarbons, n-alkanes, hopanes, levoglucosan, palmitic acid (PALMIA), stearic acid (STEARA), and cholesterol) in $PM_{2.5}$ collected in a Chinese megacity were analyzed. Source apportionment of OC was conducted by the OM-CMB approach, and then the source contributions to $PM_{2.5}$ were indirectly estimated. In addition, source apportionment of $PM_{2.5}$ was directly conducted by the IOM-CMB method, and source contributions to $PM_{2.5}$ estimated by the OM-CMB and the IOM-CMB methods were compared. Finally, the sensitivity to different source profiles for coal combustion and gasoline vehicles were tested.

2. Methodology

2.1. Sampling

$PM_{2.5}$ samples were collected from a megacity in China, Chengdu (102°54′ to 104°53′ E, 30°05′ to 31°26′ N), from January to December in 2018. Chengdu is located on the Chengdu Plain, at the western edge of the Sichuan Basin. Because of the basin's terrain and meteorology, there is an inversion layer all year round, which is not conducive to the horizontal and vertical mixing of air pollutants and it is easy to form a dense air pollution layer at the surface. As the capital of Sichuan province, Chengdu is a centre of economic development and transportation in Southwestern China, with continuous development of industry and

changes in traffic conditions.

The sampling site (Fig. S1) is at the Environmental Protection Building (EPB, 104°04′ E, 30°35′ N), which is located in a mixed residential and commercial area of the downtown city. There is no obvious industrial emission near the building. The sampling site is located on the rooftop of the EPB building, which is approximately 25 m above ground level. Daily samples were collected and the sampling duration was 22 h. The sampling was stopped during rainy days. There were a total of 64 p.m.$_{2.5}$ samples collected in 2018.

The samples were collected using two medium-volume air samplers (TH-150, Wuhan Tianhong, China) with a flow rate of 100 L/min. The sampling instrument flow was calibrated before sampling in each season, and the flow error was maintained within ±2.5%. Polypropylene (90 mm in diameter) and quartz filters (90 mm in diameter) were used to collect particulate matter. After sampling, the quartz filters were kept in aluminum foil bags and stored at −4 °C. Quartz filters were baked in an oven before use to remove organic interference.

Quartz filters were baked in an oven before use to remove organic interference. Before and after sampling, all the filters were equilibrated at the same environmental condition of constant temperature (20 ± 1 °C) and RH (50 ± 5%) for 48 h in a balance room before weighing. Each filter was weighted by a sensitive microbalance with balance sensitivity ±0.010 mg. After weighing, the loaded filters were stored at −20 °C in the fridge for the subsequent chemical analysis.

2.2. Chemical analysis and quality assurance and quality control (QA/QC)

Source specific inorganic and organic markers were analyzed, including OC, EC, ions, elements, PAHs, n-alkanes, hopane, levoglucosan, fatty acids, and cholesterol. The particles collected on the polypropylene filters were used for the analysis of elements including Si, Ca, Al by inductively coupled plasma-atomic emission spectrometer (ICP-AES) (ICAP 7400 ICP-AES; Thermo Fisher Scientific, USA). A 1/8 portion section of each polypropylene filter was cut into small pieces and placed into closed microwave digestion vessel with acid solutions (HNO_3: HCl: H_2O_2 = 1: 3: 1), then was decomposed with the microwave digestion instrument and analyzed by the ICP-AES (Feng et al., 2021).

The quartz filters were used for the analysis of the water-soluble ions (NH_4^+, Cl^-, NO_3^- and SO_4^{2-}), carbon fractions (OC and EC) and organic markers. A 1/8 portion of each quartz filter was cut and placed in a centrifuge tube with 8 ml of distilled deionized water and the solutions were refrigerated for 24 h, filtered and analyzed with a Thermo ICS900 Ion Chromatograph (Thermo Electron) (Tian et al., 2013). Carbon components including OC and EC were measured by a thermal/optical carbon aerosol analyzer (DRI, 2001A, Atmoslytic Inc.) based on the IMPROVE thermal/optical reflectance (TOR) protocol. A quartz filter of 0.588 cm^2 was heated to the temperatures of 140, 280, 480, and 580 °C to detect OC1, OC2, OC3, and OC4 in a pure helium atmosphere. Then, the temperature was increased to 540, 780, and 840 °C for EC1, EC2, and EC3 analyses in a 2% O_2 atmosphere. Organic pyrolysed carbon (OPC) was also detected after adding oxygen. According to the IMPROVE thermal/optical reflectance protocol, OC is defined as OCl+OC2+OC3 +OC4+OPC, and EC is defined as ECl+EC2+EC3-OPC.

Organic compounds, including 10 n-alkanes, 14 PAHs, 3 hopanes, 2 fatty acids, levoglucosan and cholesterol, were measured by gas chromatography-mass spectrometry (GC-MS). The full names and corresponding abbreviations of the components are summarized in Table 1. A quarter of each quartz filter was cut and put into a tube prior to analysis of PAHs, n-alkanes, and hopane. It underwent a sonicated extraction with 20 mL dichloromethane and n-hexane (v/v 1:1) under ice bath conditions twice, each for 15 min, and filtration into a round-bottomed flask by a 0.22 μm filter. After passage through a pre-activated solid phase extraction cartridge and elution with n-hexane, the solution was concentrated under reduced pressure on a rotary evaporator to near dryness (less than 5 ml), and was reduced to less than 1 ml by a slow nitrogen blow. Then, the internal standards were added to the samples and the final volumes were adjusted to 1 ml before injection in the GC. The internal standards included a mixture of naphthalene-d$_8$, acenaphthene-d$_{10}$, phenanthrene-d$_{10}$, chrysene-d$_{12}$, and perylene-d$_{12}$ (100 ng for each), 100 ng hexamethylbenzene, and 1 μg n-tetracosane-d$_{50}$.

Another quarter of the quartz filters was cut and put into tubes to analyze fatty acids and cholesterol. The 5 ml methanol and 10 ml dichloromethane (v/v 1:2) were added into the tubes and sonicated, extracted for 10 min and repeated 3 times. The solution was filtered into a round-bottomed flask using a 0.22 μm filter. After concentration by a rotary evaporator to near 5 ml, the solution was concentrated to 1 ml by a high purity nitrogen gas stream. The extract was derivatized by BSTFA

Table 1
Full names and abbreviations of the components used in the OM-CMB and IOM-CMB; and the markers for each source category (which had high MPIN values) estimated by the two methods.

Components	Abbreviations	Used in OM-CMB	marker	Used in IOM-CMB	marker
organic carbon	OC			Yes	
element carbon	EC			Yes	
ammonium	NH_4^+			Yes	
chloride	Cl^-			Yes	
nitrate	NO_3^-		SN	Yes	SN
sulfate	SO_4^{2-}		SS	Yes	SS
aluminum	Al			Yes	
silicon	Si			Yes	
calcium	Ca		RD	Yes	
polycyclic aromatic hydrocarbons	PAHs				
phenanthrene	Phe	Yes		Yes	
anthracene	Ant	Yes		Yes	
fluoranthene	Flt	Yes		Yes	
pyrene	Pyr	Yes		Yes	
benz(a)anthracene	BaA	Yes		Yes	
chrysene	Chr	Yes		Yes	
benzo(b) fluoranthene	BbF	Yes		Yes	
benzo(k) fluoranthene	BkF	Yes		Yes	
benzo(e)pyrene	BeP	Yes		Yes	
benzo(a)pyrene	BaP	Yes		Yes	
dibenz (a,h) anthracene	DBA	Yes		Yes	
Indeno (1,2,3-cd) pyrene	IPY	Yes		Yes	
benzo (ghi)perylene	BghiP	Yes	GV	Yes	GV
coronene	Cor	Yes		Yes	
hopanes					
17α(H)-22,29,30-Trisnorhopane	C27a	Yes		Yes	
17α(H),21β(H)-30-Norhopane	C29 ab	Yes	ICC	Yes	ICC
17α(H),21β(H)-hopane	C30ab	Yes	DV	Yes	DV
n-alkanes					
n-tetracosane	C24	Yes		Yes	
n-pentacosane	C25	Yes		Yes	
n-hexacosane	C26	Yes		Yes	
n-heptacosane	C27	Yes		Yes	
n-octacosane	C28	Yes		Yes	
n-nonacosane	C29	Yes		Yes	
n-Triacontane	C30	Yes		Yes	
n-hentriacontane	C31	Yes		Yes	RD
n-dotriacontane	C32	Yes		Yes	
n-tritriacontane	C33	Yes		Yes	
Others					
levoglucosan	LEVOG	Yes	BB	Yes	BB
palmitic acid	PALMIA	Yes		Yes	
stearic acid	STEARA	Yes	CK	Yes	CK
cholesterol	CHOL	Yes		Yes	

plus 1% TMCS at 70 °C for 2 h, and used for analyzing the concentrations of n-alkanoic acids and cholesterol (He et al., 2006). The internal standard (hexamethylbenzene) was added to the samples. The last quarter of the quartz filters was cut and put into a tube to analyze levoglucosan through a high-performance anion-exchange chromatography with pulsed amperometric detection (HPAEC-PAD) (Herisau, Switzerland) with a Hamilton RCX-30 250 column. The sample was extracted with 7.0 mL of deionized water and the liquid was then filtered through a 0.22 μm filter and characterized using high-performance anion-exchange chromatography with pulsed amperometric detection (HPAEC-PAD) using an anion-exchange analytical column (Carb2 150/4.0), and a guard column (Carb2 GUARD/4). The eluent A was 200 mM NaOH and 10 mM NaAc and the initial flow rate was maintained at 0.08 mL/min. The eluent B was ultrapure water and the initial flow rate was maintained at 0.42 mL/min. Column temperature is 30 °C.

The organic markers (PAHs, hopanes, n-alkanes, fatty acids and cholesterol) were analyzed by GC-MS (7890B/5977 B, Agilent, USA) using a 30 m × 0.25 mm diameter DB-5MS capillary column (0.25 μm film thickness). The carrier gas was pure helium (purity of 99.99% or more) at a constant flow rate of 1.0 mL/min. For PAHs and hopanes, inlet and transfer line temperatures were set to 230 °C and 280 °C respectively. For fatty acids and cholesterol, inlet and transfer line temperatures were set to 280 °C. For n-alkane analysis, inlet and transfer line temperatures were set to 300 °C. EI mode was used and the ionization energy level was 70eV.

Field and laboratory blanks and spiked standard recoveries were measured to correct the corresponding data. Field blanks were collected with the pump turned off during the sampling campaign and the only difference between samples and field blanks was that air was not drawn through field blanks. Then field blanks were analyzed under the same operating procedure as the samples. Different surrogate compound including each n-alkane, PAHs mixture, each hopane (O2Si Smart Solutions, USA); standards for PALMIA, STEARA, and CHOL (Dr. Ehrenstorfer, Germany); and standard for LEVOG (U.S. Pharmacopeia, USA) were added into blank samples for the determination of the recovery ratio. The recovery values of all target components showed a low relative standard deviation. In addition, the first sample of every ten samples was re-examined and the precision was found to be within 10%. The recoveries were 103.3 (mean)±5.0% (s.d.) for elements, and 105.3 ± 9.5% for ions. For carbon fractions, a system stability test (three-peak detection) is required before and after detecting samples and the relative standard deviation should not exceed 5%. The recoveries of PAHs, n-alkanes, hopanes, levoglucosan, fatty acids and cholesterol ranged from 84.7 ± 11.9%, 99.5 ± 8.3%, 110.7 ± 17.2%, 101.3 ± 0.1% and 74.9 ± 9.9%, respectively. Considering that losses of semi-volatile compounds can occur during the equilibration of quartz filters, low molecular weight PAH and n-alkane data were not utilised in this study.

In addition, the chemical species were reconstructed using the following equations referred to in the IMPROVE Report V (Hand et al., 2011):

$$\text{Ammonium sulfate} = 1.375\left[SO_4^{2-}\right] \quad (1)$$

$$\text{Ammonium nitrate} = 1.29\left[NO_3^{-}\right] \quad (2)$$

$$\text{Organic matter (OM)} = 1.8[\text{OC}] \quad (3)$$

$$\text{Crustal material} = 2.2[\text{Al}] + 2.49[\text{Si}] + 1.63[\text{Ca}] + 2.42[\text{Fe}] + 1.94[\text{Ti}] \quad (4)$$

$$\text{Other} = \text{PM} - \text{sulfate} - \text{nitrate} - \text{organic matter} - \text{crustal material} - \text{EC} \quad (5)$$

It should be noted that the average OM/OC ratios may change with locations and seasons, and the ratios can be estimated through aerosol mass spectrometer (AMS) elemental analysis (Xu et al., 2021a). Due to the lack of related data in Chengdu, the OM/OC ratio was selected as 1.8 as suggested in the IMPROVE Report V (Hand et al., 2011). The regression analysis between reconstructed $PM_{2.5}$ mass versus measured daily $PM_{2.5}$ concentrations was also used as a test (as shown in Fig. S2), indicating that they were well correlated.

2.3. Chemical mass balance (CMB) modelling

Two methods were used to conduct the source apportionment of $PM_{2.5}$. The organic marker-based CMB (OM-CMB) model was used in this study to apportion the sources of OC and $PM_{2.5}$ (Schauer et al., 1996; Villalobos et al., 2017). This model was applied to determine the primary source contributions (including gasoline vehicles, diesel vehicles, industrial coal combustion, resuspended dust, biomass burning, cooking, and vegetation detritus) to OC, and the contributions of the primary emission sources to $PM_{2.5}$ were calculated using the ratios of $PM_{2.5}$ mass to fine OC in each source. The SO_4^{2-} and NO_3^- were not included in the OM-CMB modeling, but they were measured in the profiles of above primary sources, so the contributions of secondary SO_4^{2-} and NO_3^- were calculated by the difference between the measured concentrations and the amount estimated in the primary source emissions (Zheng et al., 2002). In other words, the identified primary emissions of sulfate, nitrate ion were subtracted from measured atmospheric ionic species concentrations, and then they were converted to ammonium sulfate and ammonium nitrate using the equations (1) and (2) above. In addition, the secondary organic carbon (SOC) was considered as the unresolved source, and was calculated as the difference between measured OC and the sum of all significant contributions to OC (Villalobos et al., 2017).

For the inorganic and organic marker-based CMB (IOM-CMB) model, $PM_{2.5}$ source apportionment was conducted based on inorganic and organic source profiles as showed in Table 1. The profiles of gasoline vehicles, diesel vehicles, industrial coal combustion, resuspended dust, biomass burning, cooking, soil dust, sulfate, and nitrate were inputted into the CMB model, and their contributions were directly obtained. The SOC was also calculated as the difference between measured OC and the sum of all primary contributions to OC, and then was converted to SOA through equation (3). In addition, if the source profile of vegetation detritus is used in the IOM-CMB modeling, most outputs did not match the evaluation parameters (which are described in the following paragraph). Thus, the other difference from the OM-CMB modeling is that a soil dust profile was used in the IOM-CMB modeling. The soil dust profiles used in this study were collected from uncovered park, greenbelt, and farmland, where vegetation abounds and were strongly influenced by vegetation detritus. Although they are two different source categories, their profiles are similarly characterized by high loadings of C31 and C33 n-alkanes (Tian et al., 2021b) due to vegetation influence. Details of the source profiles used in the two methods will be discussed in Section 2.4. The components introduced into the OM-CMB and IOM-CMB are summarized in Table 1.

To ensure the reliability of the fitting results, the following reliability parameters were used to evaluate the model outputs of the two methods. The percent mass explained by the model is typically between 80 and 120%. For goodness-of-fit parameters, high r^2 (>0.8) and low χ^2 (<4) were required (Zheng et al., 2002; Lee et al., 2008; Xu et al., 2021a). In addition, the MPIN (modified pseudo inverse normalized) matrix was checked to determine the marker of each source category.

In addition, an independent estimation of the SOA was also conducted by the EC tracer method (defined as the SOA_{EC}) to compare with the SOA estimated the OM-CMB and IOM-CMB. Assuming EC totally comes from primary sources and the OC/EC ratio in primary sources is relatively constant, SOC_{EC} was estimated as in Turpin and Huntzicker (1995):

$$SOC_{EC} = OC - EC * (OC/EC)_{pri} \quad (6)$$

$$SOA_{EC} = 1.8[SOC_{EC}] \quad (7)$$

where OC and EC are the measured ambient concentrations; $(OC/EC)_{pri}$

is the OC/EC ratio in primary aerosols. Minimum R Squared (MRS) method is used to quantify $(OC/EC)_{pri}$, which has a clear quantitative criterion for the $(OC/EC)_{pri}$ calculation (Hu et al., 2012; Wu and Yu, 2016). According to Fig. S3, the $(OC/EC)_{pri}$ is 2.3 in this work.

For quantitative comparisons between the two methods, the consistency of average values was estimated by the relative biases (Equation (8)), and the consistency of temporal variations were estimated by the Pearson's r.

$$\text{Relative biases} = \frac{|C_{OM} - C_{IOM}|}{(C_{OM} + C_{IOM})/2} \quad (8)$$

2.4. Source profiles

The source profiles applied in this study include: (1) gasoline vehicles, diesel vehicles, coal combustion, resuspended dust and soil dust which were reported in our previous publication (Tian et al., 2021b); (2) biomass burning (Wang et al., 2009; Pirovano et al., 2015), cooking (Zhao et al., 2015), and vegetative detritus (Rogge et al., 1993; Hildemann et al., 1991) from other publications; and (3) ammonium sulfate and ammonium nitrate which were used to represent secondary sulfate and nitrate. To test the sensitivity of CMB results to source profiles, two different profiles of coal combustion (residential vs. industrial coal combustion as in Tian et al., 2021b) and seven different profiles of gasoline vehicles (as in Tian et al., 2021b) vs. those from U.S. non-catalyst vehicles in Schauer et al. (2002) and from Chinese gasoline vehicles in Cai et al. (2017) were evaluated for CMB modelling. Inorganic ions and elements were not showed in the Cai et al. (2017), so only OM-CMB can be compared.

3. Results and discussion

3.1. $p.m._{2.5}$ chemical composition

The daily concentrations of the $PM_{2.5}$ and mass closure of main species are shown in Fig. 1a. $PM_{2.5}$ concentrations ranged from 28 to 237 μg m^{-3}. For the mass closure of $PM_{2.5}$ chemical composition referred to the equations (1)–(5), the fractions were in the order of OM (29%) > nitrate (24%) > crustal material (23%) > sulfate (15%) > EC (5%). Furthermore, the daily concentrations of organic components are shown in Fig. 1b. Their concentrations were in the order of $\sum_{10}$n-alkanes (213 ± 73 ng m^{-3}) > levoglucosan (264 ± 208 ng m^{-3}) > $\sum$unsaturated fatty acids and cholesterol (60 ± 20 ng m^{-3}) > $\sum_{14}$PAHs (9 ± 13 ng m^{-3}) ≈ $\sum_{3}$hopanes (9 ± 5 ng m^{-3}). The concentrations of n-alkanes, levoglucosan, PAHs and hopanes showed similar temporal variations with $PM_{2.5}$ concentrations, while unsaturated fatty acids and cholesterol showed different variations. Meteorological parameters (wind speed, temperature and precipitation) for the study area are shown in Fig. S4. The concentrations of $PM_{2.5}$ and most components were higher during the dry season (Jan. to Apr., Nov. to Dec.) than during the wet season (Jun. to Oct.), due to less favorable meteorological conditions for dispersion and deposition during the dry season. Furthermore, PAHs are mainly emitted from combustion activities. Hopanes are often found in traffic exhaust and coal combustion emissions (Oros and Simoneit, 2000). N-alkanes can arise from abrasion products from vegetation leaf surfaces (characterized by the predominance of > C29 odd n-alkanes) and fossil fuel combustion (Han et al., 2018). The levoglucosan is the marker of biomass burning. The

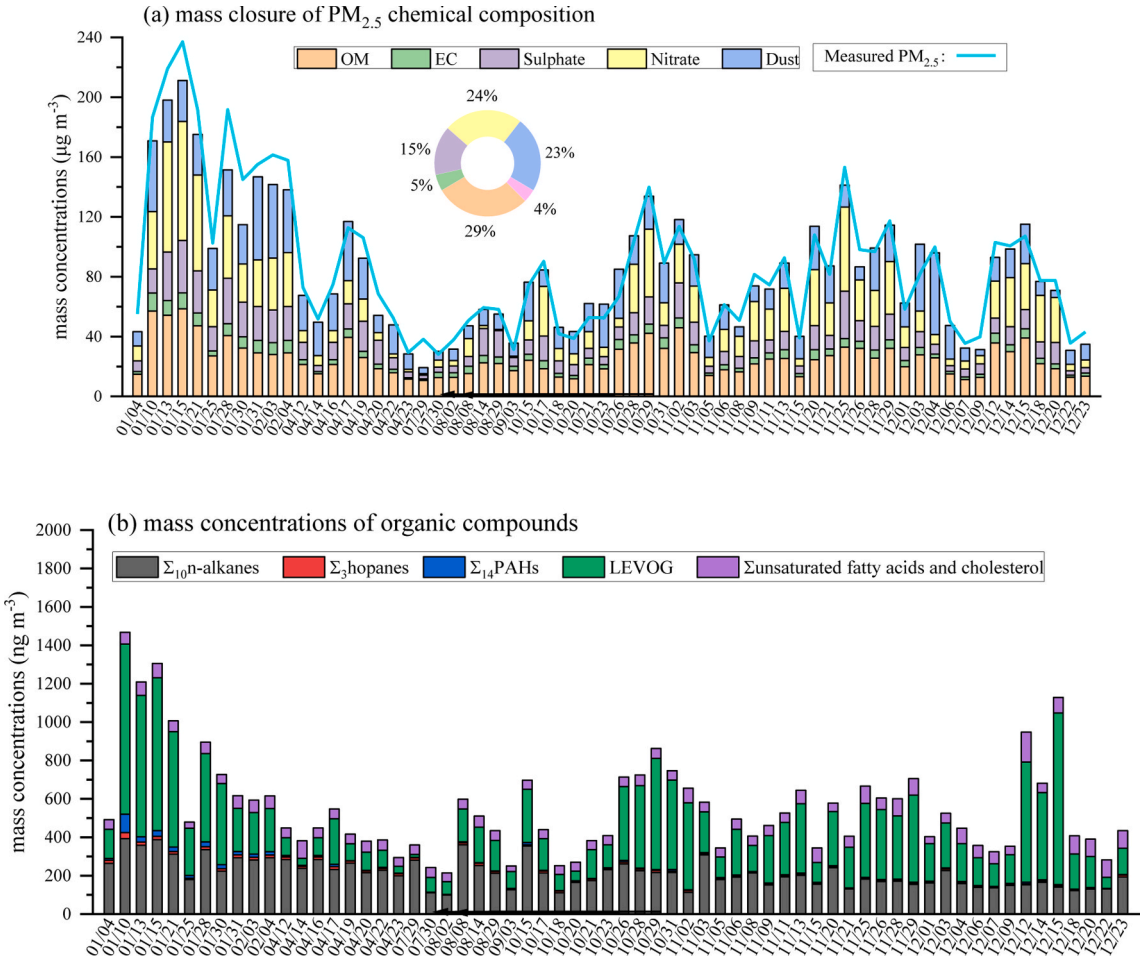

Fig. 1. (a) Daily mass closure results for $PM_{2.5}$, and daily measured concentrations of $PM_{2.5}$. (b) Daily mass concentrations of organic compounds in $PM_{2.5}$.

unsaturated fatty acids and cholesterol are usually the markers of food cooking. The temporal variations of the inorganic and organic markers can indicate the variation of source contributions.

3.2. Average source contributions to OC and $PM_{2.5}$ and comparison

The annual average of the source contributions to OC estimated by the OM-CMB is shown in Fig. 2a. The highest contributor for OC was SOC (34%), followed by biomass burning (17%), diesel vehicles (10%), industrial coal combustion (9%), gasoline vehicles (8%), resuspended dust (8%), vegetation detritus (8%), and cooking (6%). Then, as described in the methods section, for the OM-CMB model, the source contributions to $PM_{2.5}$ were converted from the contributions to OC. The average source contributions and conversion ratios are summarized in Table S1. For the IOM-CMB model, the source contributions to $PM_{2.5}$ were directly estimated. Fig. 2b and c describe the annual average source contributions to $PM_{2.5}$. The percentage contributions estimated by the OM-CMB and IOM-CMB were respectively for gasoline vehicles (4% vs 4%), diesel vehicles (10% vs 11%), industrial coal combustion (15% vs 15%), resuspended dust (12% vs 17%), biomass burning (5% vs 6%), cooking (3% vs 2%), vegetation detritus (4% vs 5%), SOA (9% vs 10%), sulfate (10% vs 7%), and nitrate (20% vs 18%).

In this study, except for the soil dust and vegetation detritus, similar source profiles were shared by the OM-CMB and IOM-CMB. A comparison of the contributions estimated by the two CMB methods was conducted, and the relative biases were calculated for comparisons, as shown in Fig. 2d. Among the primary source categories, the average contributions of the gasoline vehicles, diesel vehicles, industrial coal combustion, biomass burning and cooking estimated by the two methods were generally consistent, with the relative biases being 8.0%, 5.9%, 2.2%, 17.3% and 10.9%, while the average contributions of resuspended dust and dust/vegetation detritus showed larger differences for the two methods with relative biases being 33.3% and 26.5%. The markers for each source category which had high MPIN values estimated by the two methods are summarized in Table 1. The markers of the gasoline vehicles, diesel vehicles, industrial coal combustion, biomass burning and cooking were same in the OM-CMB and IOM-CMB, indicating that the primary sources sharing same markers in the two methods showed consistent average contributions. It can be seen that the average contributions of sulfate and nitrate from the OM-CMB were higher than those from the IOM-CMB, with the relative biases being 27.3% and 12.1%. The high relative biases may result from the fact that the sulfate and nitrate sources from the OM-CMB are the measured values after subtracting the summed mass of sulfate and nitrate emitted from the selected primary sources as described in the section 2.3, while those from the IOM-CMB were directly estimated by the CMB model. The difference of average contributions of sulfate and nitrate might be caused by uncertainties in the estimation of primary source contributions (such as in resuspended dust).

3.3. Daily contributions to OC and $PM_{2.5}$

The daily percentage contributions to OC estimated by the OM-CMB model are shown in Fig. 3a, and the daily percentage contributions to $PM_{2.5}$ estimated by the two methods are shown in Fig. 3b and c. The daily absolute contributions are shown in Fig. 4. The highest daily contributions of gasoline vehicles reached 6 μg m^{-3} for OC, and reached 21 and 20 μg m^{-3} for $PM_{2.5}$ estimated by the OM-CMB and IOM-CMB models, respectively. The percentage contributions of gasoline vehicles showed obvious higher contributions during the cold period,

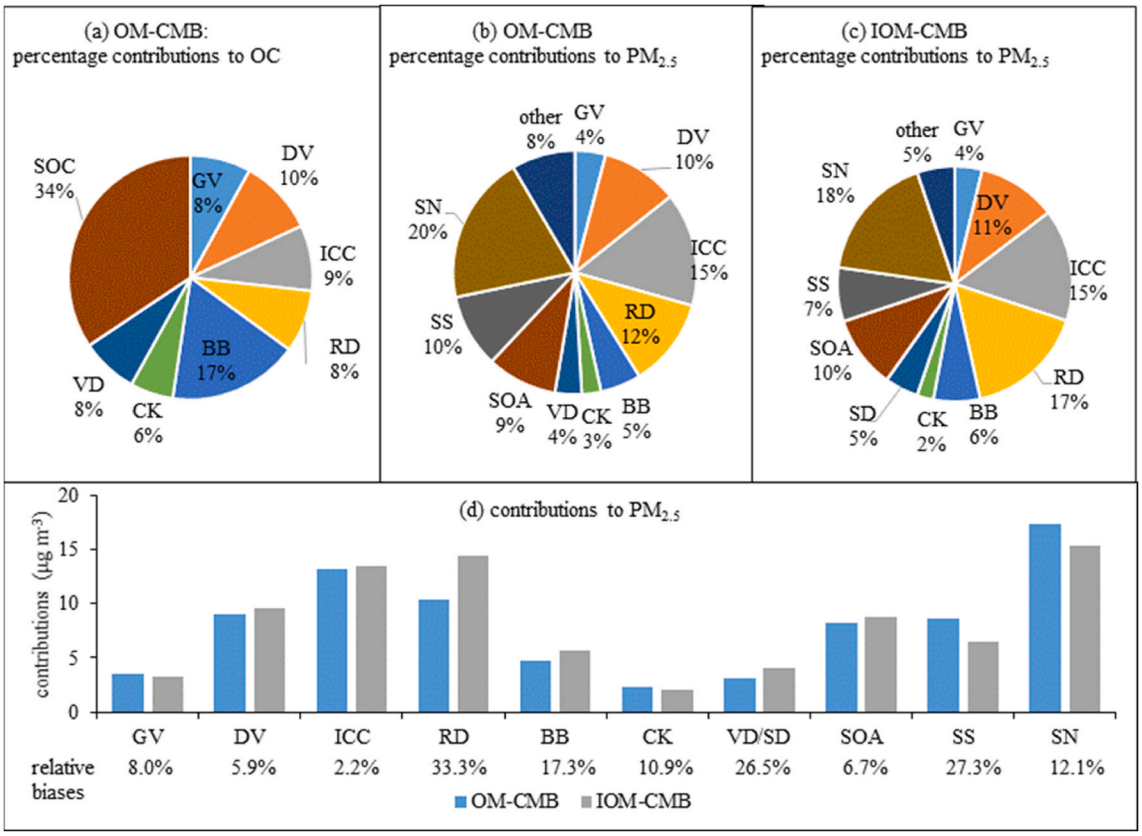

Fig. 2. (a) The average of percentage contributions to OC estimated by the OM-CMB. (b) The annual average of percentage contributions to PM2.5 estimated by the OM-CMB. (c) The annual average of percentage contributions to PM2.5 estimated by the IOM-CMB. (d) Comparison of contributions to PM2.5 estimated by the OM-CMB and IOM-CMB. GV: gasoline vehicles; DV: diesel vehicles; ICC: industrial coal combustion; RD: resuspended dust; BB: biomass burning; CK: cooking; VD: vegetation detritus; SD: soil dust; SOA: secondary organic aerosol; SS: sulfate; SN: nitrate.

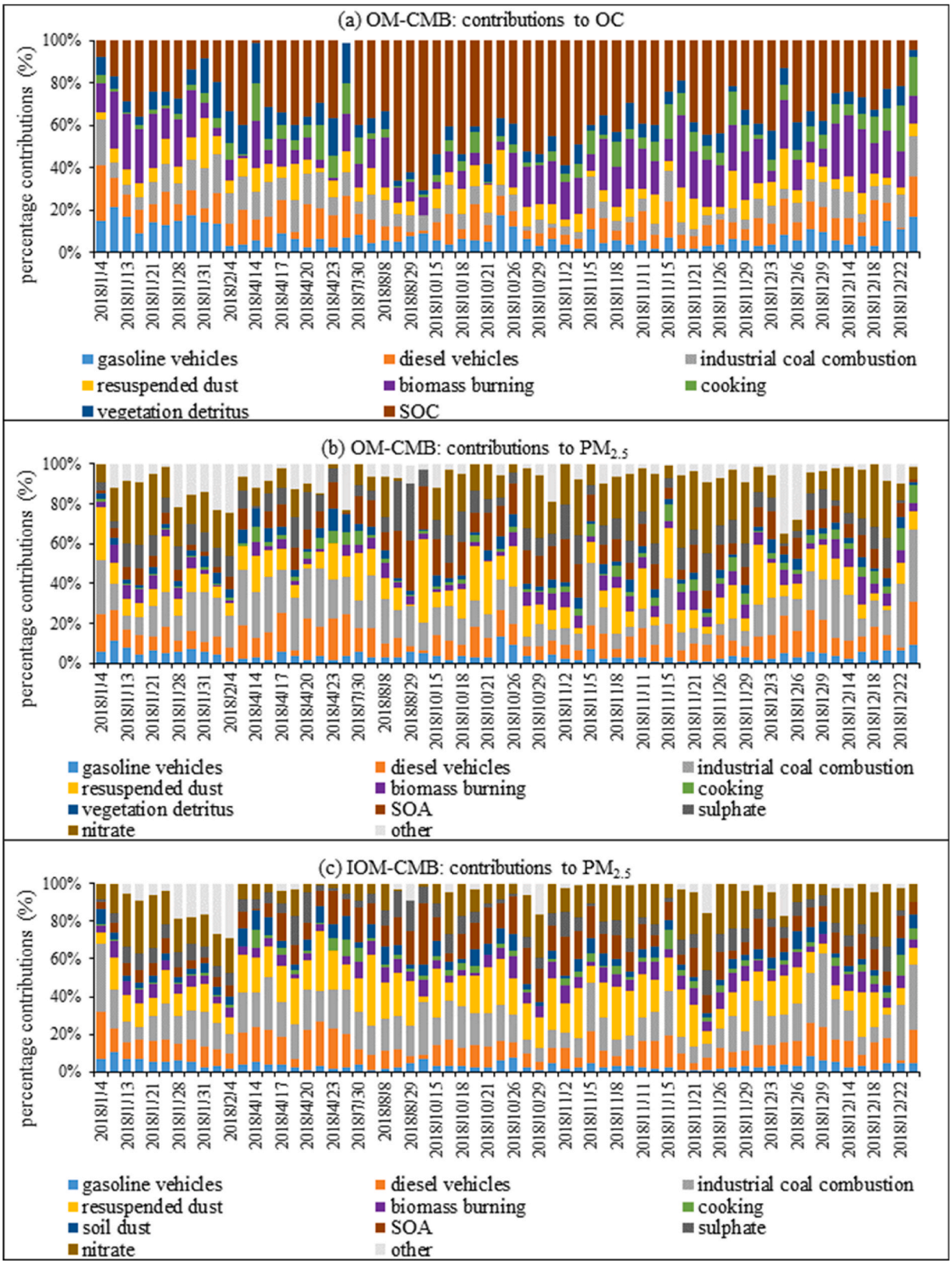

Fig. 3. (a) Daily contributions to OC estimated by the OM-CMB; (b) Daily contributions to $PM_{2.5}$ estimated by the OM-CMB; (c) Daily contributions to $PM_{2.5}$ estimated by the IOM-CMB.

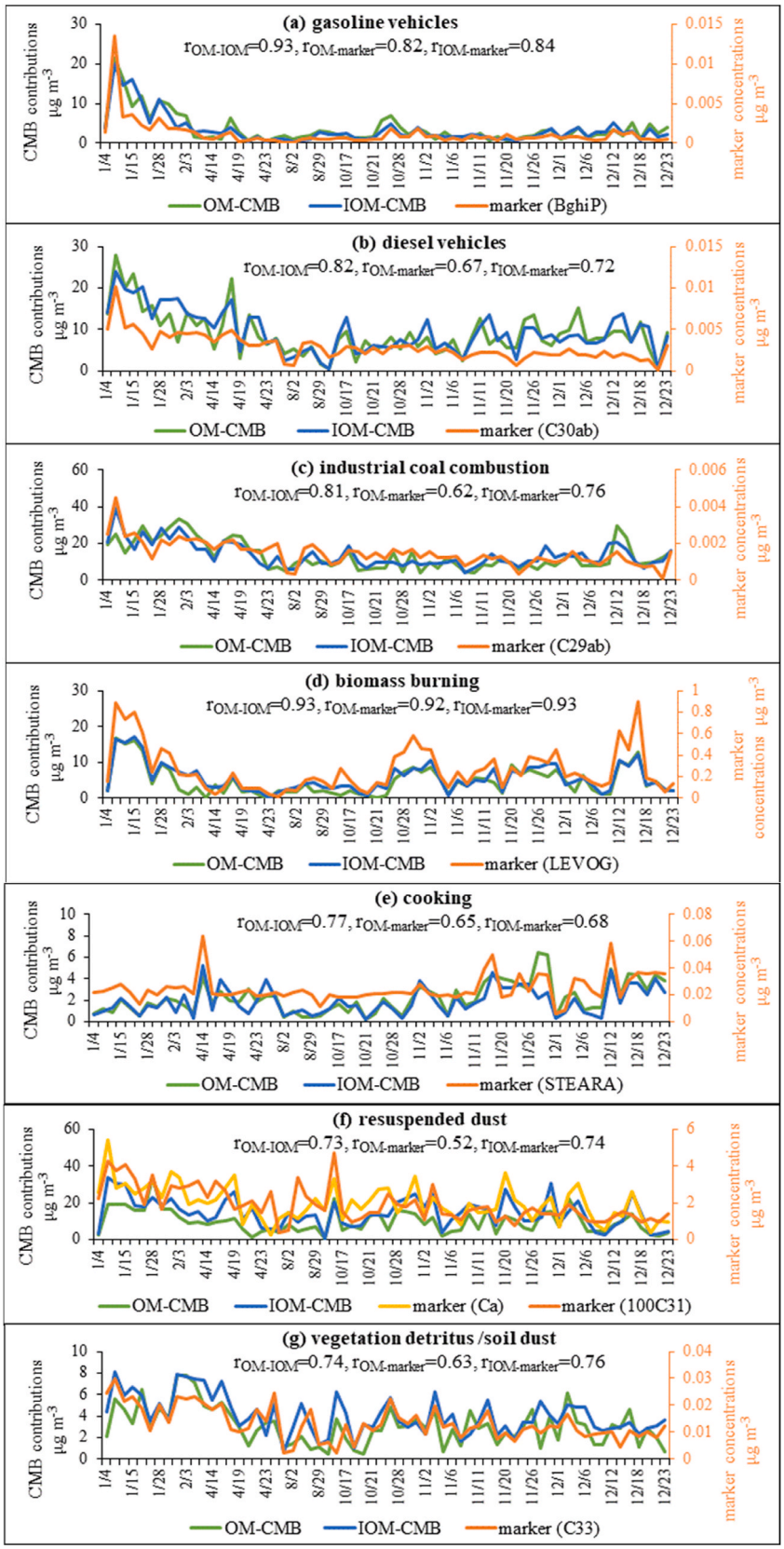

Fig. 4. Comparisons among temporal variations of source contributions estimated by the OM-CMB and IOM-CMB, and corresponding markers. rOM-IOM: Pearson's r between temporal variations of source contributions estimated by the OM-CMB and IOM-CMB methods. rOM-marker: Pearson's r between temporal variations of source contributions estimated by the OM-CMB and corresponding markers. rIOM-marker: Pearson's r between temporal variations of source contributions estimated by the IOM-CMB and corresponding markers.

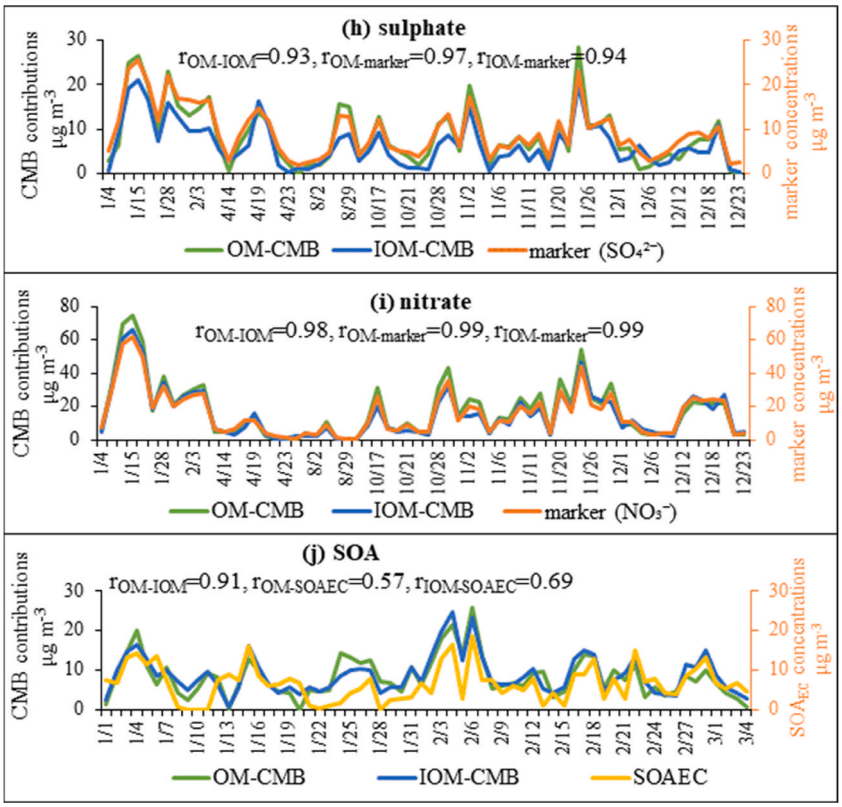

Fig. 4. (*continued*).

especially during heavy pollution in January. The highest daily contributions of diesel vehicles were 4 μg m^{-3} for OC, and 28 (OM-CMB) and 24 (IOM-CMB) μg m^{-3} for $PM_{2.5}$ which also occurred in January. Studies have shown that vehicles emit more PM under poor combustion conditions, such as cold starts at low temperature (Schauer et al., 2003). The highest industrial coal combustion contribution to OC was 3 μg m^{-3}, and to $PM_{2.5}$ reached 33 and 39 μg m^{-3}. The percentage contributions of industrial coal combustion show a slightly higher contribution in the dry season than the wet season (dry 15.3% vs. wet 13.6%), which may be the result of differing emissions or meteorology in the two seasons. Hydropower supplies a large percentage of Chengdu's electricity demand during the wet season, while coal combustion is needed for electricity generation during the dry season (Shi et al., 2016). The highest daily contributions of biomass burning can reach 8 μg m^{-3} for OC, and both 17 μg m^{-3} for $PM_{2.5}$. Biomass burning showed higher fractions during autumn (September, October and November) and winter (January, February and December), due to residential use and local straw burning activities. A high vegetation detritus/soil dust contribution was mainly observed during spring (April), while the resuspended dust showed weaker seasonal variation. According to Fig. S4, the wind speed was stronger and the precipitation was less during spring in Chengdu. Strong wind can enhance the dispersion of PM from local sources, but also can result in the resuspension of dust and vegetation detritus (Dillner et al., 2006). Dry surfaces, strong wind speeds and more vegetation impacts during spring can explain the higher contributions of vegetation detritus and soil dust (Tian et al., 2021b). The resuspended dust can be caused by high wind strength and intensive human activities (such as road dust caused by heavy traffic, construction dust caused by building activities, etc.), which can explain its weaker seasonal variation than soil dust.

The SOC was an important contributor for OC which can reach 14 μg m^{-3}, and the highest daily contributions of SOA to $PM_{2.5}$ reached 26 and 25 μg m^{-3} estimated by the OM-CMB and IOM-CMB models, respectively. The highest daily contributions to $PM_{2.5}$ reached 28 and 21 μg m^{-3} for sulfate, and 75 and 66 μg m^{-3} for nitrate, estimated by the OM-CMB and IOM-CMB models, respectively. The highest percentage contributions (%) of SOA and sulfate were observed during August to October. Their formation is associated with photochemical processes which are more efficient because of high insolation and temperatures during August to October as shown in Fig. S4 (Liu et al., 2014). The SOA and sulfate also showed higher contributions during January. Although photochemical reactions may be generally weak during January, high precursor concentrations, humidity and PM during winter may enhance the aqueous phase and heterogeneous reactions (Zhang et al., 2013; Chen et al., 2014; Cheng et al., 2016; Tian et al., 2016). The highest fraction of nitrate occurred when the temperature was low (as shown in Fig. 1). Although photochemical reactions are favorable in summer (July and August), nitrate may decompose at higher temperatures due to the thermodynamic instability of ammonium nitrate (Hasheminassab et al., 2014), and the high relative humidity during wintertime in Chengdu can enhance the secondary formation of nitrate through heterogeneous reactions (Liu et al., 2019).

3.4. Comparisons of temporal variations of source contributions and markers

The temporal variations of source contributions estimated by the OM-CMB and IOM-CMB methods were compared, and then the contributions were also compared with the corresponding markers which had high MPIN values, as shown in Fig. 4. As shown in Fig. 4 a to g, among the primary source categories, the daily variability of biomass burning and gasoline vehicles from two methods showed the most consistent temporal variations (with the Pearson's r both being 0.93 ($p < 0.01$)). The biomass burning and gasoline vehicle contributions also showed similar temporal variations with their corresponding markers, with the Pearson's r ranging from 0.82 ($p < 0.01$) to 0.93 ($p < 0.01$). The marker of gasoline vehicles was Benzo [ghi]Perylene (BghiP) and the marker of biomass burning was LEVOG, which were very different from other sources, so their low collinearity with other sources can explain the

consistent results. The temporal variations of diesel vehicles and industrial coal combustion of the two methods were moderately consistent, with the Pearson's r being 0.82 ($p < 0.01$) and 0.81 ($p < 0.01$), respectively. Consistent markers were identified for these two sources by the OM-CMB and IOM-CMB as listed in Table 1; however, the collinearity between source profiles of diesel vehicles and industrial coal combustion may cause uncertainties. For example, they are both characterized by high loadings of C24, C25 alkanes and medium-ring PAHs (Tian et al., 2021b).

According to Fig. 4e, cooking contributions estimated by the two methods showed a relatively weak correlation with each other (Pearson's $r = 0.77$, $p < 0.01$), and with the corresponding marker (Pearson's $r = 0.65$, $p < 0.01$ and 0.68, $p < 0.01$). Except for the cooking, the STEARA (marker of the cooking) also exists in the source profiles of gasoline vehicles and biomass burning. Cooking contributions were generally low, so they may be easily influenced by the gasoline vehicles and biomass burning contributions, resulting in the relatively large differences of the two methods. The contributions of resuspended dust estimated by the two methods showed high relative biases (33.3% in Fig. 2d) and relatively weak correlations (0.73, $p < 0.01$ in Fig. 4f), probably because different markers (C31 for OM-CMB and Ca for IOM-CMB) were identified for CMB modeling. The vegetation detritus from OM-CMB and the soil dust from IOM-CMB also showed high relative biases (26.5% in Fig. 2d) and weaker correlations (0.74% in Fig. 4g), because different source profiles were used in the OM-CMB and IOM-CMB modeling, although the same marker (C33) was identified for the two methods.

What's more, the temporal variations of sulfate and nitrate were highly consistent with each other and with the trends of corresponding markers with all the Pearson's r values above 0.93. The consistent temporal variations of contributions indicate they were well estimated by the two methods due to the low collinearity. As shown in Fig. 4, the temporal variations of the SOA from two methods were also strongly correlated with each other (Pearson's $r = 0.91$, $p < 0.01$). They were compared with the temporal variations of SOA_{EC} which was independently estimated by the EC tracer method as described in the method section. The Pearson's r values were 0.69 ($p < 0.01$) between SOA_{IOM} and SOA_{EC}, and were 0.57 ($p < 0.01$) between SOA_{OM} and SOA_{EC}, indicating that the SOA estimated by the IOM-CMB was more consistent with the SOA_{EC} than that estimated by the OM-CMB, because EC was used in the IOM-CMB.

3.5. Sensitivity of source apportionment to source profiles

The CMB results may vary when using different source profiles, so in this part, different profiles for two major sources - coal combustion and gasoline vehicles - were used to test the sensitivity to source profiles as mentioned above. The result of the IOM-CMB which used the residential coal combustion instead of industrial coal combustion profile is shown in Fig. 5a. Compared with the result for the industrial coal combustion, the contributions of resuspended dust and residential coal combustion were higher, and the contributions of other sources were lower. The difference between two coal combustion profiles was that the residential coal combustion showed higher OC and organic compounds and lower crustal elements than the industrial coal combustion (Tian et al., 2021b). The lower crustal elements in the residential coal combustion may explain the overestimation of the resuspended dust, whose markers were mainly crustal elements, when using its profile. Residential coal combustion is an important source category in northern China, but this is not so in the urban areas of the cities in southern China. In Chengdu, most coal is used in industrial activities, and less than 1% of coal was used for residential activities in 2018 (CBS, 2019).

For the gasoline vehicle profiles, most results did not meet the goodness-of-fit criteria when using the noncatalyst vehicle profile measured by Schauer et al. (2002). In addition, five source profiles, all from within the same study (Cai et al., 2017), and all from gasoline vehicles, but of different types, were compared in the CMB model. The results (Fig. 5b–5(f)) showed considerable sensitivity to the profile used (Tian et al., 2021b), with the gasoline vehicle contribution ranging from 1% to 8%, although changes to other source contributions were relatively small.

4. Conclusions

To explore the use of a combination of inorganic and organic markers in the CMB modeling of $PM_{2.5}$, and the influence of adopting different organic and inorganic source profiles, a comprehensive comparison of $PM_{2.5}$ source apportionment using organic marker-based OM-CMB as well as organic and inorganic marker-based IOM-CMB was conducted. The average contributions of the gasoline vehicles, diesel vehicles, industrial coal combustion, biomass burning and cooking which shared the same markers in the two methods were consistent. The average contributions of sulfate and nitrate sources showed relatively high relative biases because inorganic ions were not inputted into the OM-CMB. The temporal variations of $PM_{2.5}$ contributions from sulfate, nitrate, SOA, gasoline vehicles, and biomass burning were in good agreement between the OM-CMB and IOM-CMB results. The OM-CMB and IOM-CMB are powerful to apportion sources characterized by unique markers (such as biomass combustion) and low collinearity. The diesel vehicle and industrial coal combustion estimates were moderately consistent between the two methods. The daily contributions of resuspended dust and cooking estimated by the OM-CMB and IOM-CMB showed a poor correlation. The discrepancy in resuspended dust between OM-CMB and IOM-CMB may be due to the different tracers in their source profiles. Conceptually, the IOM-CMB model is better for apportionment of $PM_{2.5}$ as it does not depend upon the very variable sulfate and nitrate content of various primary emissions.

In addition, when testing the sensitivity to source profiles for two coal combustion and several gasoline vehicle profiles, this analysis highlights not only that CMB is quite sensitive to the source profiles used as inputs, but also that it is essential to use up-to-date local knowledge of fuels and technologies in order to obtain reliable results. In this case, the application of a source profile for industrial coal combustion and for current vehicle technologies was necessary, and the use of old or generic library source data is liable to lead to significant errors.

CMB modeling based on organic and inorganic markers is powerful for source apportionment. Identifying the source profiles that represents local sources is a core and complex effort and may limit the widespread application of this method. Furthermore, due to the possible degradation of organic molecular tracers, the use of organic tracers in receptor models can cause uncertainty. For example, studies have suggested that LEVOG can be oxidized by the OH radical (Hoffmann et al., 2010), so the biomass burning contribution will be underestimated using the LEVOG as the marker in the CMB model especially during summertime (Hennigan et al., 2010), but it is still an ideal marker compound for biomass burning due to its high emission factors and relatively high concentrations in the ambient aerosols (Hoffmann et al., 2010). In future research, the source profiles library, especially for organic compounds, should be enriched and localized to achieve more precise source appointment, and reducing the influence of degradation on the CMB modeling requires in-depth study.

CRediT authorship contribution statement

Yingze Tian: Writing – original draft, Software, Data curation. **Xiaoning Wang:** Investigation, Software. **Peng Zhao:** Investigation, Visualization. **Zongbo Shi:** Investigation. **Roy M. Harrison:** Writing – review & editing, Conceptualization.

Declaration of competing interest

The authors declare that they have no known competing financial

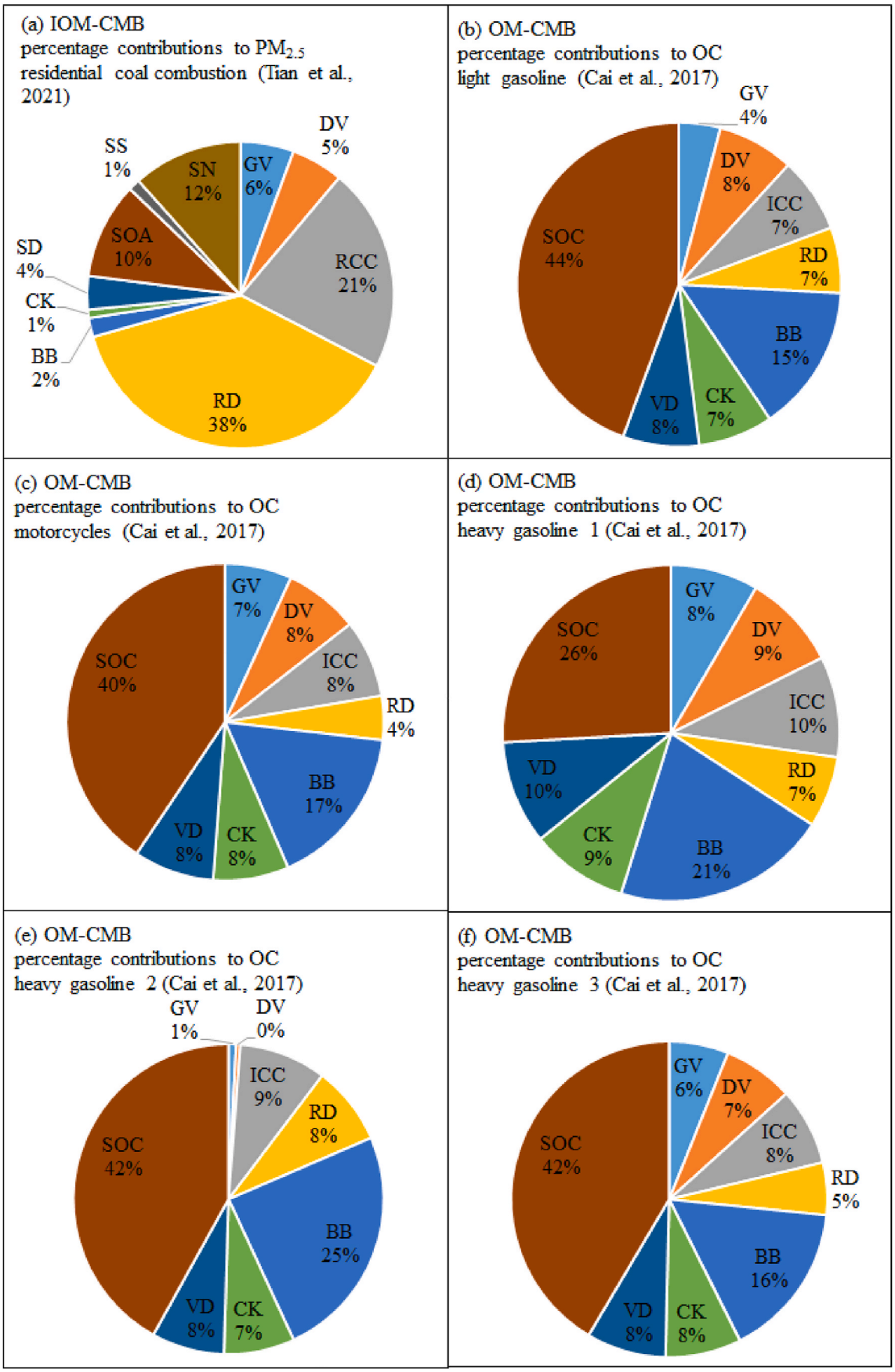

Fig. 5. (a) The result of the IOM-CMB which used the source profiles for residential coal combustion instead of industrial coal combustion measured by Tian et al. (2021b). (b) to (f) The results of the OM-CMB which used the source profiles for gasoline vehicles measured by Cai et al. (2017).

interests or personal relationships that could have appeared to influence the work reported in this paper.

Data availability

Data supporting this publication are openly available from the UBIRA eData repository at https://doi.org/10.25500/edata.bham.00000745.

Acknowledgements

This research has been supported by the National Natural Science Foundation of China, China (41977181), and Young Elite Scientists Sponsorship Program by Tianjin, China (TJSQNTJ-2018-04). RMH and ZS are supported by Natural Environment Research Council, United Kingdom (NE/N007190/1).

Appendix A. Supplementary data

Supplementary data to this article can be found online at https://doi.org/10.1016/j.atmosenv.2022.119477.

References

Aguilera, R., Corringham, T., Gershunov, A., Benmarhnia, T., 2021. Wildfire smoke impacts respiratory health more than fine particles from other sources: observational evidence from Southern California. Nat. Commun. 12, 1493. https://doi.org/10.1038/s41467-021-21708-0.

Arhami, M., Shahne, M.Z., Hosseini, V., Haghighat, N.R., Lai, A.M., Schauer, J.J., 2018. Seasonal trends in the composition and sources of $PM_{2.5}$ and carbonaceous aerosol in Tehran, Iran. Environ. Pollut. 239, 69–81.

Bell, M.L., Ebisu, K., Leaderer, B.P., Gent, J.F., Lee, H.J., Koutrakis, P., Wang, Y., Dominici, F., Peng, R.D., 2014. Associations of $PM_{2.5}$ constituents and sources with hospital admissions: analysis of four counties in Connecticut and Massachusetts (USA) for persons >= 65 years of age. Environ. Health Perspect. 122, 138–144.

Cai, T., Zhang, Y., Fang, D., Shang, J., Zhang, Y., Zhang, Y., 2017. Chinese vehicle emissions characteristic testing with small sample size: results and comparison. Atmos. Pollut. Res. 8, 154–163.

Chen, Y., Xie, S., Luo, B., 2014. Characteristics and origins of carbonaceous aerosol in the Sichuan Basin, China. Atmos. Environ. 94, 215–223.

Cheng, Y.F., Zheng, G.J., Wei, C., Mu, Q., Zheng, B., Wang, Z.B., Gao, M., Zhang, Q., He, K.B., Carmichael, G., Poschl, U., Su, H., 2016. Reactive nitrogen chemistry in aerosol water as a source of sulfate during haze events in China. Sci. Adv. 2, e1601530.

Chow, J.C., Watson, J.G., Lowenthal, D.H., Chen, L.W.A., Zielinska, B., Mazzoleni, L.R., Magliano, K.L., 2007. Evaluation of organic markers for chemical mass balance source apportionment at the Fresno Supersite. Atmos. Chem. Phys. 7, 1741–1754.

CBS, 2019. Chengdu Bureau of statistics. Chengdu 2019 Statistical Yearbook. http://www.cdstats.chengdu.gov.cn/htm/detail_333124.html.

Daellenbach, K.R., Uzu, G., Jiang, J.H., Cassagnes, L.E., Leni, Z., Vlachou, A., Stefenelli, G., Canonaco, F., Weber, S., Segers, A., 2020. Sources of particulate-matter air pollution and its oxidative potential in Europe. Nature 587, 414–419.

Dillner, A.M., Schauer, J.J., Zhang, Y.H., Zeng, L.M., Cass, G.R., 2006. Size-resolved particulate matter composition in Beijing during pollution and dust events. J. Geophys. Res. Atmos. 111, D05203 https://doi.org/10.1029/2005JD006400.

Esmaeilirad, S., Lai, A., Abbaszade, G., Schnelle-Kreis, J., Zimmermann, R., Uzu, G., Daellenbach, K., Canonaco, F., Hassankhany, H., Arhami, M., Baltensperger, U., Prevot, A.S.H., Schauer, J.J., Jaffrezo, J.L., Hosseini, V., El Haddad, I., 2020. Source apportionment of fine particulate matter in a Middle Eastern Metropolis, Tehran-Iran, using PMF with organic and inorganic markers. Sci. Total Environ. 705, 135330.

Feng, X., Tian, Y., Xue, Q., Song, D., Huang, F., Feng, Y., 2021. Measurement report: spatiotemporal and policy-related variations of $PM_{2.5}$ composition and sources during 2015-2019 at multiple sites in a Chinese megacity. Atmos. Chem. Phys. 21, 16219–16235.

Faridi, S., Yousefian, F., Roostaei, V., Harrison, R.M., Azimi, F., Niazi, S., Naddafi, K., Momeniha, F., Malkawi, M., Moh'd Safi, H.A., Rad, M.K., Hassanvand, M.S., 2022. Source apportionment, identification and characterization, and emission inventory of ambient particulate matter in 22 Eastern Mediterranean Region countries: a systematic review and recommendations for good practice. Environ. Pollut. 310, 119889.

Guo, S., Hu, M., Guo, Q., Zhang, X., Schauer, J.J., Zhang, R., 2013. Quantitative evaluation of emission controls on primary and secondary organic aerosol sources during Beijing 2008 Olympics. Atmos. Chem. Phys. 13, 8303–8314.

Han, D.M., Fu, Q.Y., Gao, S., Li, L., Ma, Y.G., Qiao, L.P., Xu, H., Liang, S., Cheng, P.F., Chen, X.J., Zhou, Y., Yu, J.Z., Cheng, J.P., 2018. Non-polar organic compounds in autumn and winter aerosols in a typical city of eastern China: size distribution and impact of gas-particle partitioning on PM2.5 source apportionment. Atmos. Chem. Phys. 18, 9375–9391.

Hand, J., Copeland, S., McDade, C., Day, D., Moore Jr., C., Dillner, A., Pitchford, M., Indresand, H., Schichtel, B., Malm, W., Watson, J., 2011. Interagency monitoring of protected visual environments (IMPROVE). In: Spatial and Seasonal Patterns and Temporal Variability of Haze and its Constituents in the United States. Report V ISSN: 0737-5352-87.

Harrison, R.M., Smith, D.J.T., Luhana, L., 1996. Source apportionment of atmospheric polycyclic aromatic hydrocarbons collected from an urban location in Birmingham, U.K. Environ. Sci. Technol. 30, 825–832.

Hasheminassab, S., Daher, N., Saffari, A., Wang, D., Ostro, B.D., Sioutas, C.m, 2014. Spatial and temporal variability of sources of ambient fine particulate matter ($PM_{2.5}$) in California. Atmos. Chem. Phys. 14, 12085–12097.

He, L.Y., Hu, M., Huang, X.F., Zhang, Y.H., Tang, X.Y., 2006. Seasonal pollution characteristics of organic compounds in atmospheric fine particles in Beijing. Sci. Total Environ. 359, 167–176.

Hildemann, L.M., Markowski, G.R., Cass, G.R., 1991. Chemical composition of emissions from urban sources of fine organic aerosol. Environ. Sci. Technol. 25, 744–759.

Hoffmann, D., Tilgner, A., Iinuma, Y., Herrmann, H., 2010. Atmospheric stability of levoglucosan: a detailed laboratory and modeling study. Environ. Sci. Technol. 44, 694–699.

Hennigan, C.J., Sullivan, A.P., Collett, J.L., Robinson, A.L., 2010. Levoglucosan stability in biomass burning particles exposed to hydroxyl radicals. Geophys. Res. Lett. 37, L09806.

Hu, W.W., Hu, M., Deng, Z.Q., Xiao, R., Kondo, Y., Takegawa, N., Zhao, Y.J., Guo, S., Zhang, Y.H., 2012. The characteristics and origins of carbonaceous aerosol at a rural site of PRD in summer of 2006. Atmos. Chem. Phys. 12, 1811–1822.

Huang, R.J., Zhang, Y.L., Bozzetti, C., Ho, K.F., Cao, J.J., Han, Y.M., Daellenbach, K.R., Slowik, J.G., Platt, S.M., Canonaco, F., Zotter, P., Wolf, R., Pieber, S.M., Bruns, E.A., Crippa, M., Ciarelli, G., Piazzalunga, A., Schwikowski, M., Abbaszade, G., Schnelle-Kreis, J., Zimmermann, R., An, Z.S., Szidat, S., Baltensperger, U., El Haddad, I., Prevot, A.S.H., 2014. High secondary aerosol contribution to particulate pollution during haze events in China. Nature 514, 218–222.

Ke, L., Liu, W., Wang, Y., Russell, A.G., Edgerton, E.S., Zheng, M., 2008. Comparison of $PM_{2.5}$ source apportionment using positive matrix factorization and molecular marker-based chemical mass balance. Sci. Total Environ. 394, 290–302.

Lee, S., Liu, W., Wang, Y.H., Russell, A.G., Edgerton, E.S., 2008. Source apportionment of $PM_{2.5}$: comparing PMF and CMB results for four ambient monitoring sites in the southeastern United States. Atmos. Environ. 42, 4126–4137.

Li, X., Yan, C., Wang, C., Ma, J., Li, W., Liu, J., Liu, Y., 2022. $PM_{2.5}$-bound elements in Hebei Province, China: pollution levels, source apportionment and health risks. Sci. Total Environ. 806, 150440.

Li, L., Li, Q., Huang, L., Wang, Q., Zhu, A.S., Xu, J., Liu, Z.Y., Li, H.L., Shi, L.S., Li, R., Azari, M., Wang, Y.J., Zhang, X.J., Liu, Z.Q., Zhu, Y.H., Zhang, K., Xue, S.H., Ooi, M.C.G., Zhang, D.P., Chan, A., 2020. Air quality changes during the COVID-19 lockdown over the Yangtze River Delta Region: an insight into the impact of human activity pattern changes on air pollution variation. Sci. Total Environ. 732, 139282.

Liu, F., Tan, Q., Jiang, X., Yang, F., Jiang, W., 2019. Effects of relative humidity and $PM_{2.5}$ chemical compositions on visibility impairment in Chengdu, China. J. Environ. Sci. 86, 15–23.

Liu, J.W., Li, J., Zhang, Y.L., Liu, D., Ding, P., Shen, C.D., Shen, K.J., He, Q.F., Ding, X., Wang, X.M., Chen, D.H., Szidat, S., Zhang, G., 2014. Source apportionment using radiocarbon and organic tracers for $PM_{2.5}$ carbonaceous aerosols in Guangzhou, South China: contrasting local- and regional-scale haze events. Environ. Sci. Technol. 48, 12002–12011.

Liu, Q.Y., Baumgartner, J., Zhang, Y., Schauer, J.J., 2016. Source apportionment of Beijing air pollution during a severe winter haze event and associated pro-inflammatory responses in lung epithelial cells. Atmos. Environ. 126, 28–35.

Lu, Z.J., Liu, Q.Y., Xiong, Y., Huang, F., Zhou, J.B., Schauer, J.J., 2018. A hybrid source apportionment strategy using positive matrix factorization (PMF) and molecular marker chemical mass balance (MM-CMB) model. Environ. Pollut. 238, 39–51.

Mancilla, Y., Medina, G., Gonzalez, L.T., Herckes, P., Fraser, M.P., Mendoza, A., 2021. Determination and similarity analysis of $PM_{2.5}$ emission source profiles based on organic markers for Monterrey, Mexico. Atmosphere 12, 554. https://doi.org/10.3390/atmos12050554.

Marmur, A., Park, S.K., Mulholland, J.A., Tolbert, P.E., Russell, A.G., 2006. Source apportionment of $PM_{2.5}$ in the southeastern United States using receptor and emissions-based models: conceptual differences and implications for time-series health studies. Atmos. Environ. 40, 2533–2551.

McDuffie, E.E., Martin, R.V., Spadaro, J.V., Burnett, R., Smith, S.J., O'Rourke, P., Hammer, M.S., van Donkelaar, A., Bindle, L., Shah, V., Jaegle, L., Luo, G., Yu, F.Q., Adeniran, J.A., Brauer, M., 2021. Source sector and fuel contributions to ambient $PM_{2.5}$ and attributable mortality across multiple spatial scales. Nat. Commun. 12, 3594. https://doi.org/10.1038/s41467-021-23853-y.

Oros, D.R., Simoneit, B.R.T., 2000. Identification and emission rates of molecular tracers in coal smoke particulate matter. Fuel 79, 515–536.

Pereira, G.M., Teinila, K., Custodio, D., Santos, A.G., Xian, H., Hillamo, R., Alves, C.A., Andrade, J.B.D., Rocha, G.O.D., Kumar, P., Balasubramanian, R., Andrade, M.D.F., Vasconcellos, P.D.C., 2017. Particulate pollutants in the Brazilian city of Sao Paulo: 1-year investigation for the chemical composition and source apportionment. Atmos. Chem. Phys. 17, 11943–11969.

Perrone, M.G., Larsen, B.R., Ferrero, L., Sangiorgi, G., De Gennaro, G., Udisti, R., Zangrando, R., Gambaro, A., Bolzacchini, E., 2012. Sources of high $PM_{2.5}$ concentrations in Milan, Northern Italy: molecular marker data and CMB modelling. Sci. Total Environ. 414, 343–355.

Pirovano, G., Colombi, C., Balzarini, A., Riva, G.M., Gianelle, V., Lonati, G., 2015. $PM_{2.5}$ source apportionment in Lombardy (Italy): comparison of receptor and chemistry-transport modelling results. Atmos. Environ. 106, 56–70.

Robinson, A.L., Subramanian, R., Donahue, N.M., Bernardo-Bricker, A., Rogge, W.F., 2006. Source apportionment of molecular markers and organic aerosol. 3. Food cooking emissions. Environ. Sci. Technol. 40, 7820–7827.
Robinson, A.L., Donahue, N.M., Shrivastava, M.K., Weitkamp, E.A., Sage, A.M., Grieshop, A.P., Lane, T.E., Pierce, J.R., Pandis, S.N., 2007. Rethinking organic aerosols: semivolatile emissions and photochemical aging. Science 315, 1259–1262.
Rogge, W.F., Hildemann, L.M., Mazurek, M.A., Cass, G.R., Simoneit, B., 1993. Sources of fine organic aerosol. 4. Particulate abrasion products from leaf surfaces of urban plants. Environ. Sci. Technol. 27, 2700–2711.
Schauer, J.J., 2003. Evaluation of elemental carbon as a marker for diesel particulate matter. J. Expo. Anal. Environ. Epidemiol. 13, 443–453.
Schauer, J.J., Kleeman, M.J., Cass, G.R., Simoneit, B.R.T., 2002. Measurement of emissions from air pollution sources. 5. C-1-C-32 organic compounds from gasoline-powered motor vehicles. Environ. Sci. Technol. 36, 1169–1180.
Schauer, J.J., Cass, G.R., 2000. Source apportionment of wintertime gas-phase and particle-phase air pollutants using organic compounds as tracers. Environ. Sci. Technol. 34, 1821–1832.
Schauer, J.J., Rogge, W.F., Hildemann, L.M., Mazurek, M.A., Cass, G.R., 1996. Source apportionment of airborne particulate matter using organic compounds as tracers. Atmos. Environ. 30, 3837–3855.
Shi, G.L., Peng, X., Liu, J.Y., Tian, Y.Z., Song, D.L., Yu, H.F., Feng, Y.C., Russell, A.G., 2016. Quantification of long-term primary and secondary source contributions to carbonaceous aerosols. Environ. Pollut. 219, 897–905.
Song, L., Dai, Q., Feng, Y., Hopke, P.K., 2021. Estimating uncertainties of source contributions to $PM_{2.5}$ using moving window evolving dispersion normalized PMF. Environ. Pollut. 286, 117576.
Thurston, G.D., Chen, L.C., Campen, M., 2022. Particle toxicity's role in air pollution. Science 375, 506-506.
Tian, S.L., Pan, Y.P., Wang, Y.S., 2016. Size-resolved source apportionment of particulate matter in urban Beijing during haze and non-haze episodes. Atmos. Chem. Phys. 1–19.
Tian, Y.Z., Harrison, R.M., Feng, Y.C., Shi, Z.B., Liang, Y.L., Li, Y.X., Xue, Q.Q., Xu, J.S., 2021a. Size-resolved source apportionment of particulate matter from a megacity in northern China based on one-year measurement of inorganic and organic components. Environ. Pollut. 289, 117932.
Tian, Y.Z., Liu, X., Huo, R.Q., Shi, Z.B., Sun, Y.M., Feng, Y.C., Harrison, R.M., 2021b. Organic compound source profiles of $PM_{2.5}$ from traffic emissions, coal combustion, industrial processes and dust. Chemosphere 278, 130429.
Tian, Y.Z., Shi, G.L., Han, S.Q., Zhang, Y.F., Feng, Y.C., Liu, G.R., Gao, L.J., Wu, J.H., Zhu, T., 2013. Vertical characteristics of levels and potential sources of water-soluble ions in PM10 in a Chinese megacity. Sci. Total Environ. 447, 1–9.
Turpin, B.J., Huntzicker, J.J., 1995. Identification of secondary organic aerosol episodes and quantitation of primary and secondary organic aerosol concentrations during SCAQS. Atmos. Environ. 29, 3527–3544.
Villalobos, A.M., Barraza, F., Jorquera, H., Schauer, J.J., 2017. Wood burning pollution in southern Chile: $PM_{2.5}$ source apportionment using CMB and molecular markers. Environ. Pollut. 225, 514–523.
Wang, Q., Shao, M., Zhang, Y., Wei, Y., Hu, M., Guo, S., 2009. Source apportionment of fine organic aerosols in Beijing. Atmos. Chem. Phys. 9, 9043–9080.
Wen, J., Chuai, X., Gao, R., Pang, B., 2022. Regional interaction of lung cancer incidence influenced by PM2.5 in China. Sci. Total Environ. 803, 149979.
Weber, R., 2020. A map of potentially harmful aerosols in Europe. Nature 587, 369–370.
Wong, Y.K., Huang, X.H.H., Cheng, Y.Y., Yu, J.Z., 2021. Estimating primary vehicular emission contributions to $PM_{2.5}$ using the Chemical Mass Balance model: accounting for gas-particle partitioning of organic aerosols and oxidation degradation of hopanes. Environ. Pollut. 291, 118131.
Wu, X.F., Chen, C.R., Vu, T.V., Liu, D., Baldo, C., Shen, X.B., Zhang, Q., Cen, K., Zheng, M., He, K.B., Shi, Z.B., Harrison, R.M., 2020. Source apportionment of fine organic carbon (OC) using receptor modelling at a rural site of Beijing: Insight into seasonal and diurnal variation of source contributions. Environ. Pollut. 266, 115078.
Wu, C., Yu, J.Z., 2016. Determination of primary combustion source organic carbon-to-elemental carbon (OC/EC) ratio using ambient OC and EC measurements: secondary OC-EC correlation minimization method. Atmos. Chem. Phys. 16, 5453–5465.
Xu, J.S., Liu, D., Wu, X.F., Vu, T., Zhang, Y.L., Fu, P.Q., Sun, Y.L., Xu, W.Q., Zheng, B., Harrison, R.M., Shi, Z.B., 2021a. Source apportionment of fine organic carbon at an urban site of Beijing using a chemical mass balance model. Atmos. Chem. Phys. 21, 7321–7341.
Xu, J.S., Srivastava, D., Wu, X.F., Hou, S.Q., Vu, T.V., Liu, D., Sun, Y.L., Vlachou, A., Moschos, V., Salazar, G., Szidat, S., Prevot, A.S.H., Fu, P.Q., Harrison, R.M., Shi, Z.B., 2021b. An evaluation of source apportionment of fine OC and $PM_{2.5}$ by multiple methods: APHH-Beijing campaigns as a case study. Faraday Discuss 226, 290–313.
Yin, J., Cumberland, S.A., Harrison, R.M., Allan, J., Young, D.E., Williams, P.I., Coe, H., 2015. Receptor modelling of fine particles in southern England using CMB including comparison with AMS-PMF factors. Atmos. Chem. Phys. 15, 2139–2158.
Zhang, R., Jing, J., Tao, J., Hsu, S.C., Wang, G., Cao, J., Lee, C.S.L., Zhu, L., Chen, Z., Zhao, Y., Shen, Z., 2013. Chemical characterization and source apportionment of $PM_{2.5}$ in Beijing: seasonal perspective. Atmos. Chem. Phys. 13, 7053–7074.
Zhao, X.Y., Hu, Q.H., Wang, X.M., Ding, X., He, Q.F., Zhang, Z., Shen, R.Q., Lu, S.J., Liu, T.Y., Fu, X.X., Chen, L.G., 2015. Composition profiles of organic aerosols from Chinese residential cooking: case study in urban Guangzhou, south China. J. Atmos. Chem. 72, 1–18.
Zhao, P.S., Dong, F., He, D., Zhao, X.J., Zhang, X.L., Zhang, W.Z., Yao, Q., Liu, H.Y., 2013. Characteristics of concentrations and chemical compositions for $PM_{2.5}$ in the region of Beijing, Tianjin, and Hebei, China. Atmos. Chem. Phys. 13, 4631–4644.
Zheng, M., Salmon, L.G., Schauer, J.J., Zeng, L.M., Kiang, C.S., Zhang, Y.H., Cass, G.R., 2005. Seasonal trends in $PM_{2.5}$ source contributions in Beijing, China. Atmos. Environ. Times 39, 3967–3976.
Zheng, M., Cass, G.R., Schauer, J.J., Edgerton, E.S., 2002. Source apportionment of $PM_{2.5}$ in the Southeastern United States using solvent-extractable organic compounds as tracers. Environ. Sci. Technol. 36, 2361–2371.